Available online at www.sciencedirect.com
SCIENCE DIRECT®
Journal of Sound and Vibration 260 (2003) 369–387
JOURNAL OF SOUND AND VIBRATION
www.elsevier.com/locate/jsvi

Letter to the Editor

Dynamic analysis of a rectangular plate subjected to multiple forces moving along a circular path

Jia-Jang Wu*

Department of Marine Engineering, National Kaohsiung Institute of Marine Technology, No. 142, Hai-Chuan Road, Nan-Tzu, Kaohsiung 811, Taiwan, Republic of China

Received 2 April 2002; accepted 30 May 2002

1. Introduction

Vibration of structures due to various moving loads is an important problem in engineering, therefore, plenty of literature concerning this topic can be found. For example, Lin and Trethewey [1,2] have performed the dynamic analyses of beams and the high-speed precision drilling machine due to moving loads. Hino et al. [3–5] and Chang and Liu [6] have investigated the forced vibration responses of non-linear beams subjected to moving loads using the Galerkin method and finite element method. Wu and Dai [7] and Lee [8] have studied the dynamic behaviour of multi-span beams undergoing moving forces. Thambiratnam and Zhuge [9] have investigated the dynamic responses of elastically supported beams due to moving loads. Wu et al. [10] have presented a technique, based on the finite element method, for calculating the dynamic responses of structures due to two-dimensional moving forces. Wu et al. [11] have performed the forced vibration analyses of a flat plat subjected to various moving loads by means of the finite element method and the Newmark direct integration method. Manoach [12] has studied the dynamic behaviour of elastoplastic thick circular plates subjected to different types of pulses by using the Mindlin plate theory. Frỳba [13], Gbadeyan and Oni [14] and Lin [15] have investigated the dynamic behaviour of beams and plates undergoing moving forces and moving masses. Takabatake [16] has presented a simplified analytical method for calculating the dynamic responses of a rectangular plate with stepped thickness and subjected to moving loads. By considering the bridge as a structure composed of rectangular plates, Marchesiello et al. [17] and Zhu and Law [18] have studied the dynamic behaviour of bridges under moving vehicle loads. Rossi [19] has studied the forced vibration responses of a rectangular plate subjected to a stationary distributed harmonic loading. Shadnam et al. [20] have formulated the forced vibration problem of a rectangular plate due to a *single* force (or mass) moving along an arbitrary trajectory theoretically; however, only the case of a rectangular plate subjected to a *single* force (or mass)

*Corresponding author. Tel.: +886-7-3617141; fax: +886-6-2808458.
E-mail address: jjangwu@mail.nkimt.edu.tw (J.-J. Wu).

PII: S0022-460X(02)01009-X

moving along a *straight* path was studied by means of the analytical and numerical approaches. From the review of the existing literature, one sees that no information concerning the forced vibration analysis of plates subjected to *multiple* forces moving along a *circular* path can be obtained. For this reason, the title problem is studied in this paper.

Fig. 1(a) illustrates a rotating mechanism used in the places where rotation of object about an axis is required. Relevant examples include the modern revolving restaurant built at the top of a building so that the customers can view the beautiful scene from various directions during the meals, the revolving carriers in the entertainment centres, the revolving glass disk in the microwave oven, etc.

For the revolving glass disk of a microwave oven, the sketch for the construction of the rotating mechanism is like that shown in Fig. 1(a) and the corresponding mathematical model may be represented by Fig. 1(b). Thus, for the dynamic analysis of the rectangular bottom plate, one may model the whole system as a rectangular flat plate subjected to multiple forces moving along a circular path.

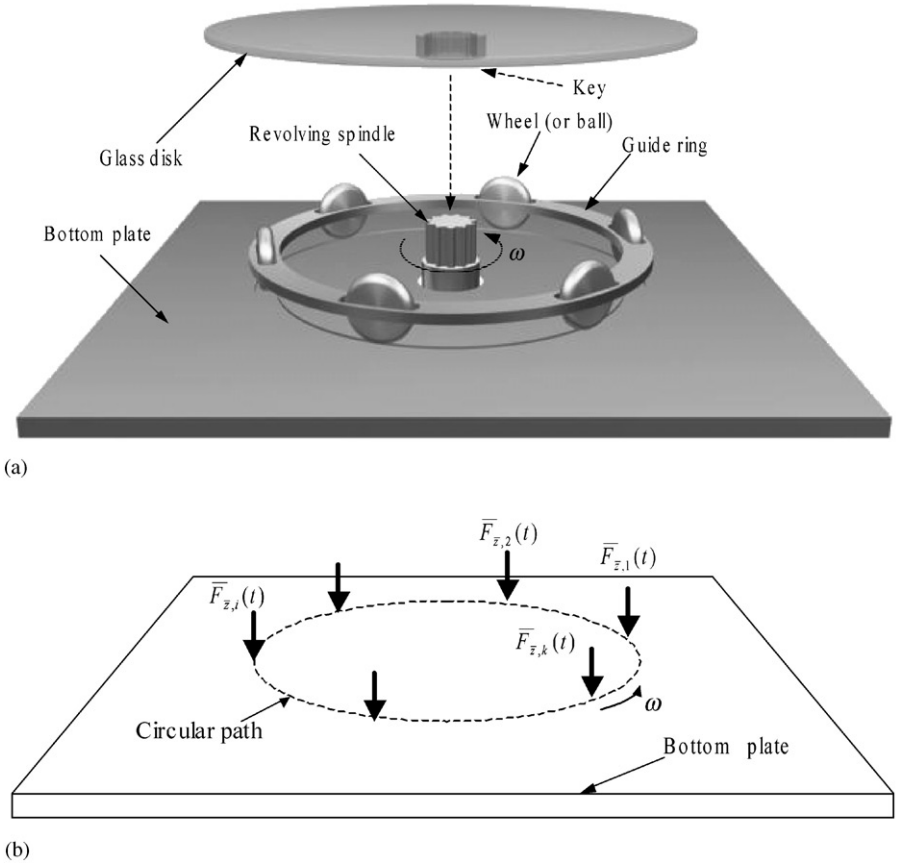

Fig. 1. (a) Sketch for the construction of the rotating mechanism and (b) the corresponding mathematical model for the dynamic analysis of the rectangular bottom plate.

When the forced vibration analyses of structures due to moving loads are performed by means of the finite element method [21], one requires to replace the external force with the equivalent nodal forces (and moments) at any instant of time t. Therefore, the formulations for calculating the instantaneous positions of the moving forces and the expressions for transforming the external loads to the equivalent nodal forces (and moments) on the structure are presented. The key point of this paper is to investigate the influence of the following factors on the dynamic behaviour of the rectangular plate: the supporting conditions of the plate, rotating speed of the moving loads, radius of the circular path, total number of the moving loads, etc.

2. Instantaneous positions of the moving loads

Fig. 2 shows a rectangular plate subjected to multiple forces, $\bar{F}_{\bar{z},i}(t)$ $(i = 1-k)$, moving, with constant rotating speed ω, along a circular path (i.e., the dashed circle with centre at $G[\bar{x}_G, \bar{y}_G]$ and radius r). If the position vectors for the moving forces are equally spaced with angle α and the angle between the position vector for the first moving force, $\bar{F}_{\bar{z},1}(t)$, and the $\bar{x}$-axis, at time $t = 0$, is denoted by θ_0, then the $\bar{x}$ and $\bar{y}$ co-ordinates for the instantaneous positions of the ith moving force, at any time t, are respectively given by

$$\bar{C}^{(s)}_{\bar{x},i}(t) = \bar{x}_G + r\cos[\theta_0 + \omega t + (i-1)\alpha], \tag{1}$$

$$\bar{C}^{(s)}_{\bar{y},i}(t) = \bar{y}_G + r\sin[\theta_0 + \omega t + (i-1)\alpha], \tag{2}$$

$$\alpha = 2\pi/k, \tag{3}$$

where k represents the total number of the moving forces.

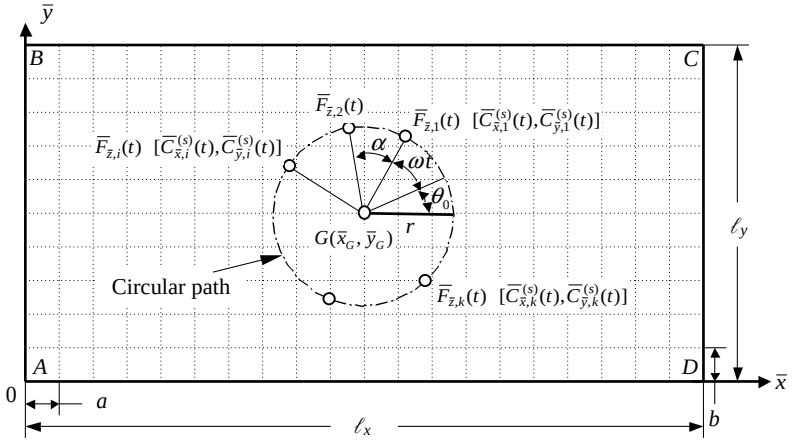

Fig. 2. A rectangular plate subjected to multiple forces, $\bar{F}_{\bar{z},i}(t)$ $(i = 1-k)$, moving along a circle with radius r and centre at point $G(\bar{x}_G, \bar{y}_G)$ with constant rotating speed ω.

For the special case of one force moving along the circular path, Eqs. (1) and (2) reduce to

$$\bar{C}^{(s)}_{\bar{x},1}(t) = \bar{x}_G + r\cos(\theta_0 + \omega t), \tag{4}$$

$$\bar{C}^{(s)}_{\bar{y},1}(t) = \bar{y}_G + r\sin(\theta_0 + \omega t). \tag{5}$$

3. Overall nodal force vector for a rectangular plate subjected to an arbitrary concentrated force

In order to solve the title problem by means of the finite element method (FEM), the continuum rectangular plate (see Fig. 3(a)) is replaced by a discrete one composed of $m \times n$ identical rectangular plate elements with $(m+1)\times(n+1)$ nodes. If the length and width of the rectangular plate are denoted by ℓ_x and ℓ_y, respectively, then those of each rectangular plate element are given by $a = \ell_x/m$ and $b = \ell_y/n$, respectively. In Fig. 3(a), the digits in the circles and parentheses, respectively, represent the numberings for the nodes and the plate elements. If, at an instant of time t, a concentrated force $P(t)$, located at the position $[\bar{C}^{(s)}_{\bar{x}}(t), \bar{C}^{(s)}_{\bar{y}}(t)]$, applies on the sth element of the rectangular plate as shown in Fig. 3(a), then the equivalent nodal forces (and moments) for the sth rectangular plate element are shown in Fig. 3(b). In Fig. 3(a), $\bar{C}^{(s)}_{\bar{x}}(t)$ and $\bar{C}^{(s)}_{\bar{y}}(t)$ are the co-ordinates of force $P(t)$ with respect to the global $\bar{x}\bar{y}$ co-ordinate system, while, in Fig. 3(b), $C^{(s)}_x(t)$ and $C^{(s)}_y(t)$ are the co-ordinates of force $P(t)$ with respect to the local xy co-ordinate system for the sth rectangular plate element. For convenience, the right superscript s, for the symbols $C_x(t)$, $C_y(t)$, $\bar{C}_{\bar{x}}(t)$ and $\bar{C}_{\bar{y}}(t)$, is used to denote the position of the concentrated force $P(t)$ applying on the sth rectangular plate element. For the relationship between the local co-ordinates $[C_x(t), C_y(t)]$ and global co-ordinates $[\bar{C}_{\bar{x}}(t), \bar{C}_{\bar{y}}(t)]$, one may refer to Eqs. (15a) and (15b).

The equation of motion for a vibrating system is given by [22]

$$[M]\{\ddot{q}(t)\} + [C]\{\dot{q}(t)\} + [K]\{q(t)\} = \{F(t)\}, \tag{6}$$

where $[M]$, $[C]$ and $[K]$ are, respectively, the overall mass, damping and stiffness matrices, $\{\ddot{q}(t)\}$, $\{\dot{q}(t)\}$ and $\{q(t)\}$ are, respectively, the nodal acceleration, velocity and displacement vectors for the whole plate, and $\{F(t)\}$ is the external force vector.

As shown in Fig. 3(a), if the rectangular plate is subjected to a concentrated force $P(t)$, the external forces on all the nodes of the plate are equal to zero except the four nodes of the sth rectangular plate element on which the concentrated force $P(t)$ applies. Thus, the external force vector $\{F(t)\}$ in Eq. (6) takes the form

$$\{F(t)\} = \begin{matrix}[0 & \dots & f^{(s)}_1(t) & f^{(s)}_2(t) & f^{(s)}_3(t) & f^{(s)}_4(t) & f^{(s)}_5(t) & f^{(s)}_6(t)\\ & & f^{(s)}_7(t) & f^{(s)}_8(t) & f^{(s)}_9(t) & f^{(s)}_{10}(t) & f^{(s)}_{11}(t) & f^{(s)}_{12}(t)\\ & & f^{(s)}_{13}(t) & f^{(s)}_{14}(t) & f^{(s)}_{15}(t) & f^{(s)}_{16}(t) & f^{(s)}_{17}(t) & f^{(s)}_{18}(t)\\ & & f^{(s)}_{19}(t) & f^{(s)}_{20}(t) & f^{(s)}_{21}(t) & f^{(s)}_{22}(t) & f^{(s)}_{23}(t) & f^{(s)}_{24}(t) & \dots & 0]^{\mathrm{T}}\end{matrix} \tag{7}$$

where

$$\{f^{(s)}(t)\}_{24\times 1} = [f^{(s)}_1(t) \quad f^{(s)}_2(t) \quad f^{(s)}_3(t) \quad \cdots \quad f^{(s)}_{24}(t)]^{\mathrm{T}} = P(t)\{N(x,y)\}, \tag{8}$$

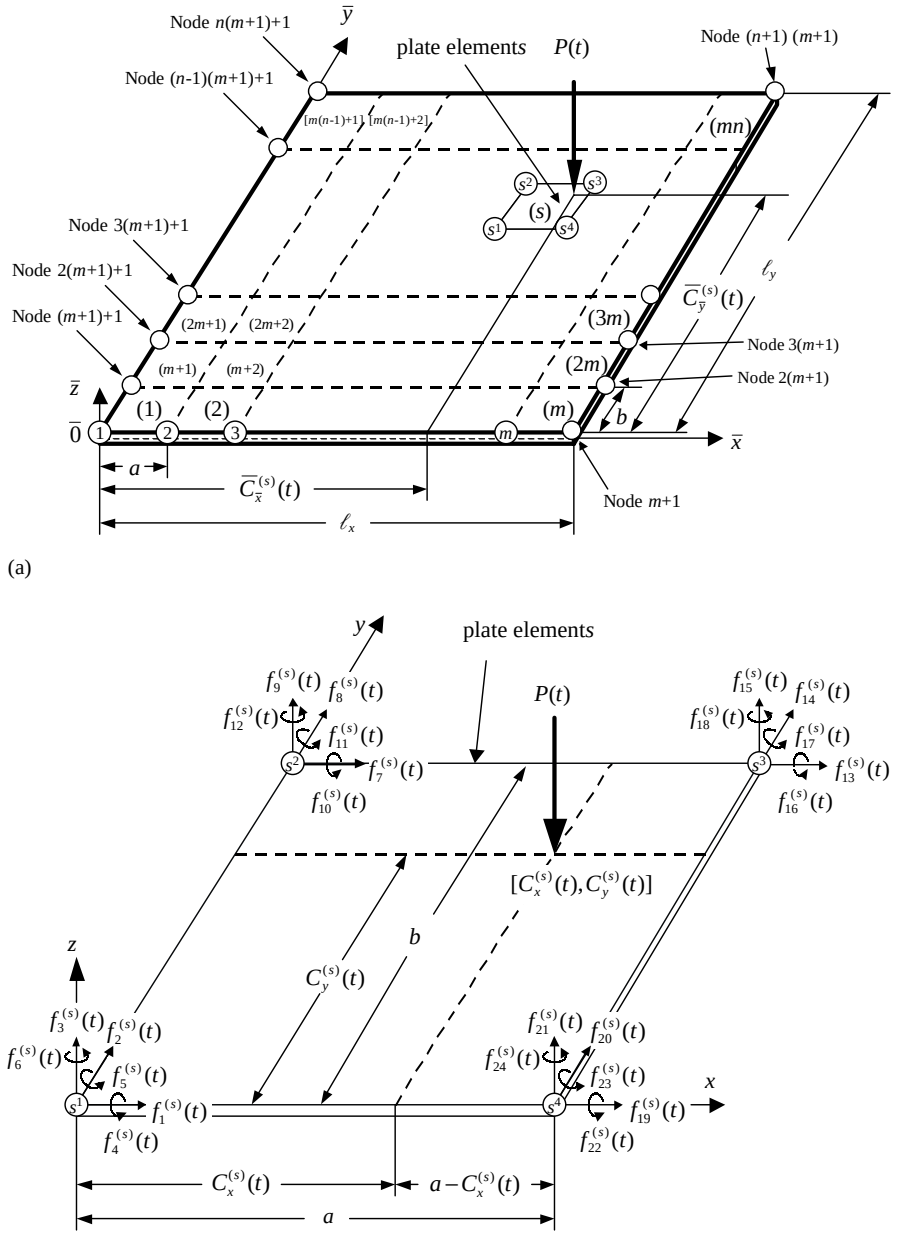

Fig. 3. (a) A rectangular plate composed of $m\times n$ plate elements and $(m+1)\times(n+1)$ nodes; (b) the equivalent nodal forces and moments corresponding to the external force $P(t)$ applied on the sth plate element.

$$\{N(x,y)\} = [\,N_1(x,y) \quad N_2(x,y) \quad \cdots \quad N_{24}(x,y)\,]^{\mathrm{T}}. \tag{9}$$

In Eqs. (7)–(9), $f_i^{(s)}(t)$ $(i=1-24)$ represent the nodal forces (or moments) equivalent to the external concentrated force $P(t)$ located at $x=C_x^{(s)}(t)$ and $y=C_y^{(s)}(t)$, while $N_i(x,y)$ $(i=1-24)$

denote the shape functions of the plate element given by [11]

$$
\begin{aligned}
N_3(x,y) &= N_3(\varsigma,\eta) = (1+2\varsigma)(1-\varsigma)^2(1+2\eta)(1-\eta)^2,\\
N_4(x,y) &= N_4(\varsigma,\eta) = (1+2\varsigma)(1-\varsigma)^2\eta(1-\eta)^2 b,\\
N_5(x,y) &= N_5(\varsigma,\eta) = -(1-\varsigma)^2\varsigma(1+2\eta)(1-\eta)^2 a,\\
N_9(x,y) &= N_9(\varsigma,\eta) = (1+2\varsigma)(1-\varsigma)^2(3-2\eta)\eta^2,\\
N_{10}(x,y) &= N_{10}(\varsigma,\eta) = -(1+2\varsigma)(1-\varsigma)^2(1-\eta)\eta^2 b,\\
N_{11}(x,y) &= N_{11}(\varsigma,\eta) = -\varsigma(1-\varsigma)^2(3-2\eta)\eta^2 a,\\
N_{15}(x,y) &= N_{15}(\varsigma,\eta) = (3-2\varsigma)\varsigma^2(3-2\eta)\eta^2,\\
N_{16}(x,y) &= N_{16}(\varsigma,\eta) = -(3-2\varsigma)\varsigma^2(1-\eta)\eta^2 b,\\
N_{17}(x,y) &= N_{17}(\varsigma,\eta) = (1-\varsigma)\varsigma^2(3-2\eta)\eta^2 a,\\
N_{21}(x,y) &= N_{21}(\varsigma,\eta) = (3-2\varsigma)\varsigma^2(1+2\eta)(1-\eta)^2,\\
N_{22}(x,y) &= N_{22}(\varsigma,\eta) = (3-2\varsigma)\varsigma^2\eta(1-\eta)^2 b,\\
N_{23}(x,y) &= N_{23}(\varsigma,\eta) = (1-\varsigma)\varsigma^2(1+2\eta)(1-\eta)^2 a,\\
N_i(x,y) &= N_i(\varsigma,\eta) = 0, \quad i = 1,2,6,7,8,12,13,14,18,19,20,24,
\end{aligned}
\tag{10}
$$

$$\varsigma = x/a = C_x^{(s)}(t)/a, \tag{11a}$$

$$\eta = y/b = C_y^{(s)}(t)/b. \tag{11b}$$

It is noted that the parameters ς and η, in Eq. (10), are functions of time t if the co-ordinates for the application point of the external concentrated force $P(t)$, $C_x^{(s)}(t)$ and $C_y^{(s)}(t)$, change from time to time.

Theoretically, if the mesh for the finite element model of the plate is very fine and the concentrated force moves from node to node in each time interval, then it is not necessary to calculate the equivalent nodal force using the foregoing shape functions because, in such a case, the magnitude of the equivalent nodal force is equal to that of the concentrated force. However, for an engineer, the general approach given by Eqs. (7)–(11) will be better than a special approach, because a general approach is suitable for most of the general cases and a special approach is usually only suitable for a few particular problems. Furthermore, the total degree of freedom for the whole system increases dramatically when very fine meshes are used, particularly for the plate elements (comparing with the beam elements).

4. Overall nodal force vector for a rectangular plate subjected to multiple forces moving along a circle

If the forces $\bar{F}_{\bar{z},i}(t)$ $(i = 1-k)$ moving along a circular path (with radius r) on the rectangular plate with constant rotating speed ω, as shown in Fig. 2, then the relationship between the time interval Δt, total time steps q, and the time duration for calculating the forced vibration responses,

t_{max}, is given by

$$t_{max} = q\,\Delta t. \tag{12}$$

At any time $t = r\,\Delta t$ ($r = 0-q$), the global co-ordinates for the instantaneous position of the ith moving force $\bar{F}_{\bar{z},i}(t)$ on the rectangular plate are given by Eqs. (1)–(3). Therefore, the numbering for the sth plate element on which the ith moving force $\bar{F}_{\bar{z},i}(t)$ applies (at time t) is determined by

$$s = [\text{Integer part of } \bar{C}^{(s)}_{\bar{y},i}(t)/b] \times m + [\text{Integer part of } \bar{C}^{(s)}_{\bar{x},i}(t)/a] + 1. \tag{13}$$

The numberings for the four nodes of the sth rectangular plate element, $s = 1$ to $m \times n$, are given by (see Fig. 3(b)):

$$\begin{aligned} s^1 &= s + (\text{Integer part of } \bar{C}^{(s)}_{\bar{y},i}(t)/b), \\ s^2 &= s^1 + (m+1), \\ s^3 &= s^1 + (m+1) + 1, \\ s^4 &= s^1 + 1 \end{aligned} \tag{14}$$

Based on the foregoing information concerning the numbering of the sth plate element and the numberings for the four nodes of the sth plate element, one may determine the nodal forces (and moments) on the sth plate element ($s = 1$ to $m \times n$) at any time $t = r\Delta t$ ($r = 0-q$) by using the shape functions given by Eqs. (10) and (11).

It is noted that the local co-ordinates, $[C^{(s)}_{x,i}(t),\ C^{(s)}_{y,i}(t)]$ given by Eqs. (11a) and (11b), instead of the global co-ordinates, $[\bar{C}^{(s)}_{\bar{x},i}(t),\ \bar{C}^{(s)}_{\bar{y},i}(t)]$ given by Eqs. (1)–(3), are used to calculate the equivalent nodal forces (and moments). The relationship between the local co-ordinates $[C^{(s)}_{x,i}(t), C^{(s)}_{y,i}(t)]$ and the global co-ordinates $[\bar{C}^{(s)}_{\bar{x},i}(t), \bar{C}^{(s)}_{\bar{y},i}(t)]$ for the instantaneous application point of the ith moving force $\bar{F}_{\bar{z},i}(t)$ is given by

$$C^{(s)}_{x,i}(t) = \bar{C}^{(s)}_{\bar{x},i}(t) - (\text{Integer part of } \bar{C}^{(s)}_{\bar{x},i}(t)/a) \times a, \tag{15a}$$

$$C^{(s)}_{y,i}(t) = \bar{C}^{(s)}_{\bar{y},i}(t) - (\text{Integer part of } \bar{C}^{(s)}_{\bar{y},i}(t)/b) \times b. \tag{15b}$$

Using the foregoing formulations one may obtain the instantaneous nodal force vector of the rectangular plate subjected to the ith moving force and assembly of all the instantaneous nodal force vectors associated with all the moving forces $\bar{F}_{\bar{z},i}(t)$ ($i = 1-k$) moving along the circular path will determine the overall instantaneous external nodal force vector $\{F(t)\}$ required by Eq. (6). From the last descriptions, it is evident that the formulation for calculating the overall nodal force vector of the plate due to a *single* force moving along the circle is only a special case of that due to the *multiple* ones.

5. Dynamic analysis of the rectangular plate

Now, the dynamic responses of a rectangular plate undergoing multiple forces moving along a circular path may be performed. First of all, the continuous rectangular plate is replaced by a discrete system so that a finite element model of the rectangular plate may be established. Then, the natural frequencies and mode shapes of the plate are calculated by using the Lanczos

algorithm [23], meanwhile, the instantaneous overall nodal force vector of the entire rectangular plate due to the forces $\bar{F}_{\bar{z},i}(t)$ $(i = 1-k)$ moving along a circle are determined using the formulations of the last section. Finally, one may use the mode superposition method and the Duhamel integration [22] to determine the dynamic responses of the plate. For the details, please refer to Ref. [7].

6. Numerical results and discussions

Fig. 2 shows the uniform undamped rectangular plate studied. The dimensions of the plate are: length $\ell_x = 2.0\,\text{m}$, width $\ell_y = 1.0\,\text{m}$ and thickness $h = 0.01\,\text{m}$. The entire plate is modelled with 200 rectangular plate elements and 231 nodes, the length and width of each rectangular plate element are: $a = b = 0.1\,\text{m}$. The plate is made of steel with mass density $\rho = 7820\,\text{kg/m}^3$ (or mass per unit area $\mu_p = 78.2\,\text{kg/m}^2$), modulus of elasticity $E = 206.8\ \text{GN/m}^2$ and the Poisson ratio $v = 0.29$. For convenience, the last rectangular plate with left side AB and right side CD hinged is called H-plate and with left side AB and right side CD clamped is called C-plate, hereafter. It is evident that, for the H-plate, all the translational degrees of freedom (d.o.f) for the boundary nodes (i.e., the nodes on side AB, and those on side CD) are constrained except that the d.o.f of rotations about the $\bar{y}$-axis are free, while, for the C-plate, all the d.o.f. associated with the above-mentioned boundary nodes are constrained.

If the mechanism shown in Fig. 1(a) may be replaced by the mathematical model shown in Fig. 1(b) and all the wheels (or balls) are equally spaced (by angle α) along the guide ring (with radius r), then the forces on the rectangular plate due to the weight of the disk together with the weight of the object on the disk will be uniformly distributed and given by

$$\bar{F}_{\bar{z},i} = F_g/k, \quad i = 1, 2, 3, \ldots, k, \tag{16}$$

where

$$F_g = \sum_{i=1}^{k} \bar{F}_{\bar{z},i} \tag{17}$$

represents the weight of the disk and the weight of the object on the disk.

It is assumed, in this paper, that the damping ratio is 0.0 for each mode and the mode number used for calculating the forced vibration responses is 10. In addition, the centre of the circular path is coincident with the centre of the rectangular plate, G, with global co-ordinates $(\bar{x}_G, \bar{y}_G)$, as one may see from Fig. 2. Furthermore, the forces $(\bar{F}_{i,\bar{z}},\ i = 1-k)$ move only in the first 10 s and then keep stationary thereafter.

Unless specially stated, the time interval $\Delta t = 0.001\,\text{s}$ and the total time steps $q = t_{\max}/\Delta t$ are used in the integration procedure, where t_{max} represents the time duration for calculating the forced vibration responses.

6.1. Free vibration analysis of the rectangular plate

In this paper, the forced vibration responses of the rectangular plates due to the moving loads are determined with the mode superposition method and the Duhamel integration [22], thus the

natural frequencies and the corresponding mode shapes of the rectangular plates at each specified supporting conditions must be calculated first. Since the total mode used for the superposition in this paper is 10, only the lowest 10 natural frequencies for the hinged–hinged plate (i.e., H-plate) and those for the clamped–clamped plate (i.e., C-plate) are listed in Table 1, where the digits listed in the 2nd and 4th columns are the natural frequencies obtained using the Lanczos algorithm [23] and those listed in 3rd and 5th columns are the natural frequencies obtained using the Jacobi method [24]. From the table, it is seen that the natural frequencies obtained from the Lanczos algorithm are very close to the corresponding ones obtained from the Jacobi method. Thus, it is believed that the last results are viable and will be used to the forced vibration analysis in this paper.

For convenience of the subsequent descriptions, the corresponding lowest two mode shapes for the H-plate and those for the C-plate are also shown in Figs. 4 and 5, respectively. It is noted that the first mode shapes for the H-plate and the C-plate are the amplitudes due to free flexural vibrations of the rectangular plates in the vertical ($\bar{z}$) directions as one may see from Figs. 4(a) and 5(a); however, the second mode shapes for the H-plate and the C-plate are those due to free torsional (or twisting) vibrations of the plates about the *line nodes MN* as shown in Figs. 4(b) and 5(b).

6.2. Responses of the rectangular plate due to a single force moving along a circle

In this subsection, the H-plate subjected to a sinusoidal force $\bar{F}_{\bar{z},1}(t) = F_{\bar{z},1} \times \sin \Omega t = 10 \times \sin \Omega t$ N moving along a circular path with radius $r = 0.3$ m, (cf., Fig. 2) is studied. Since the co-ordinates for the centre (G) of the circular path are $\bar{x}_G = 1.0$ m and $\bar{y}_G = 0.5$ m, while the initial angle between the position vector for the moving force $\bar{F}_{\bar{z},1}(t)$ and the $\bar{x}$-axis is $\theta_0 = 0$ at time $t = 0$, the global co-ordinates for the initial position of the sinusoidal force $\bar{F}_{\bar{z},1}(t)$ are given by

$$[\bar{C}^{(s)}_{\bar{x},1}(0),\ \bar{C}^{(s)}_{\bar{y},1}(0)] = [\bar{x}_G + r\cos(\theta_0 + \omega t),\ \bar{y}_G + r\sin(\theta_0 + \omega t)] = [1.3,\ 0.5]. \tag{18}$$

Table 1
The lowest 10 natural frequencies of H-plate and C-plate

Mode number	Natural frequencies, ω_i (Hz)			
	H-plate		C-plate	
	Lanczos	Jacobi	Lanczos	Jacobi
1st	5.8876	5.8905	13.6396	13.6465
2nd	16.8193	16.8278	21.9251	21.9362
3rd	23.8545	23.8665	37.7177	37.7368
4th	39.3539	39.3738	50.2198	50.2425
5th	54.1362	54.1636	65.1489	65.1819
6th	62.9348	62.9667	74.3587	74.3964
7th	71.1742	71.2103	88.3792	88.4239
8th	86.9126	86.9566	93.7498	93.7973
9th	96.8821	96.9312	123.6543	123.7161
10th	113.9956	114.0537	133.6762	133.7439

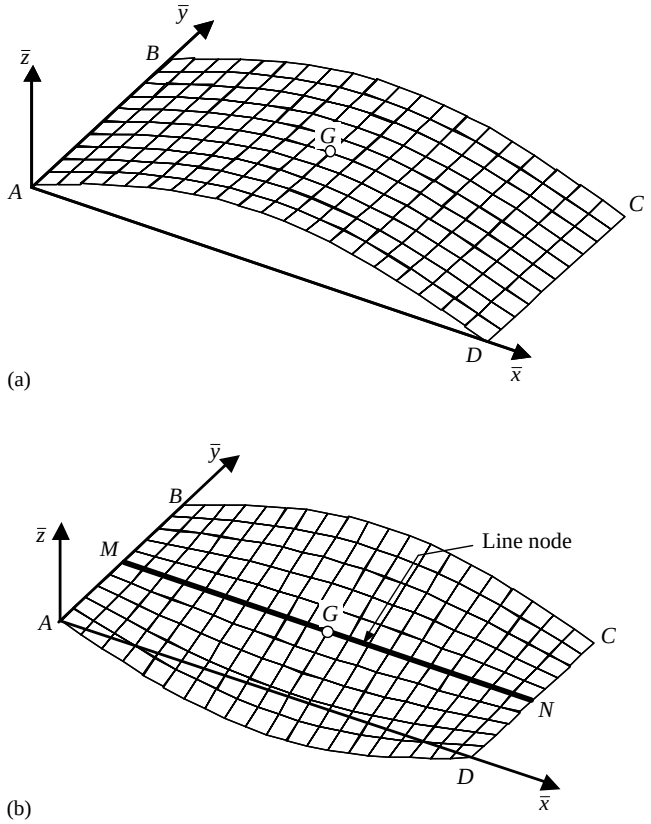

Fig. 4. Mode shapes for the hinged–hinged plate (H-plate): (a) first mode and (b) second mode.

In other words, from the point with $\bar{x} = 1.3\,\text{m}$ and $\bar{y} = 0.5\,\text{m}$, the sinusoidal force $\bar{F}_{\bar{z},1}(t) = 10 \times \sin \Omega t$ N moves along the circular path counter-clockwise, with a constant rotating speed ω rad/s, for 10 s and then stays at the instantaneous position with the instantaneous magnitude remaining unchanged, i.e., for $t \geqslant 10\,\text{s}$, one has

$$[\bar{C}^{(s)}_{\bar{x},1}(t),\ \bar{C}^{(s)}_{\bar{y},1}(t)] = [\bar{C}^{(s)}_{\bar{x},1}(10),\ \bar{C}^{(s)}_{\bar{y},1}(10)]$$
$$= [\bar{x}_G + r\cos(\theta_0 + 10\omega),\ \bar{y}_G + r\sin(\theta_0 + 10\omega)], \tag{19}$$

$$\bar{F}_{\bar{z},1}(t) = \bar{F}_{\bar{z},1}(10) = 10 \sin 10\Omega\,\text{N} = \textit{Constant}. \tag{20}$$

The time histories for the vertical ($\bar{z}$) displacements of centre G of the H-plate are shown in Fig. 6(a) when $\omega = \Omega = 5.8876\,\text{Hz} = 36.9741\,\text{rad/s}$ and in Fig. 6(b) when $\omega = \Omega = 16.8193\,\text{Hz} = 105.625\,\text{rad/s}$. A comparison between Fig. 6(a) and (b) reveals that the rotating speed ω and the forcing frequency Ω have a close relationship with the dynamic response of the rectangular plate, particularly when they are close to certain lowest natural frequencies of the plate.

For Fig. 6(a), since both the rotating speed ω and the forcing frequency Ω are equal to the first natural frequency of the H-plate ($\omega_1 = 5.8876\,\text{Hz}$), the response amplitude increases with the

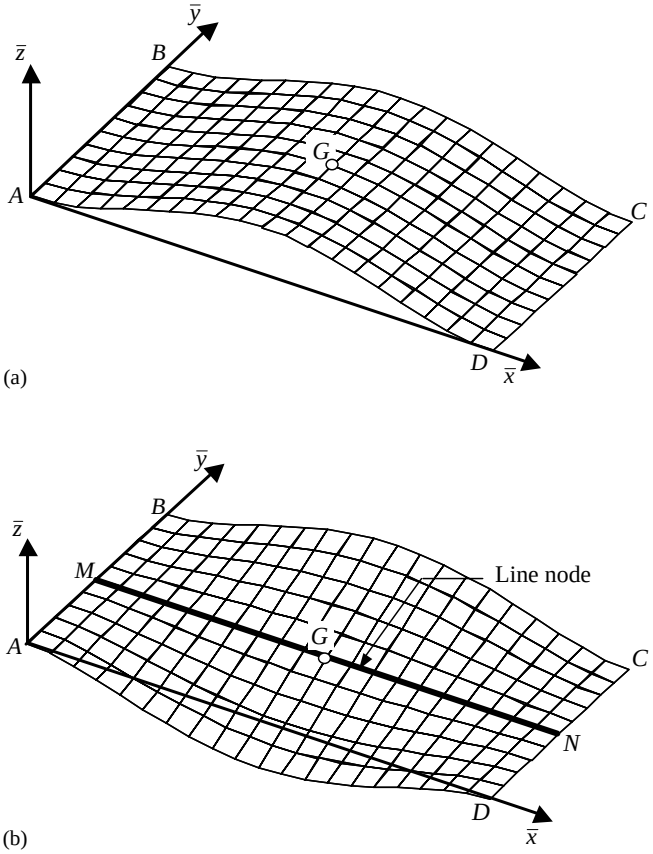

Fig. 5. Mode shapes for the clamped-clamped plate (C-plate): (a) first mode and (b) second mode.

increase of time t in the first 10 s due to undamped forced vibrations and then keeps unchanged after 10 s (i.e., $t > 10$ s) due to undamped free vibrations. Either forced or free vibration responses for the centre G of the rectangular plate are approximately symmetric with respect to the static equilibrium position of the centre G represented by the dashed line shown in Fig. 6(a). These are reasonable results, because the centre G of the H-plate is located at the crest of the first mode shape as shown in Fig. 4(a) and the resonant responses (due to $\Omega = \omega = \omega_1$) are much greater than the differential shift of the static equilibrium positions of the centre G of the H-plate due to different applying positions of the single moving load $\bar{F}_{\bar{z},1}(t)$.

For Fig. 6(b), although both the rotating speed ω and the forcing frequency Ω are equal to the second natural frequency of the H-plate ($\omega_2 = 16.8193$ Hz), the response amplitude does not increase with the increase of time t for the first 10 s. This is because the centre G of the rectangular plate is located on the line node of the second (torsional) mode shape (see Fig. 4(b)) so that the maximum central vertical ($\bar{z}$) displacement of point G is very small and any small responses of the plate will reach this maximum value. After 10 s (i.e., $t > 10$ s), the point G freely oscillates with respect to the static equilibrium position represented by the horizontal dashed line of Fig. 6(b). In Fig. 6(b), the deviation (or shift) between the horizontal solid line (with respect to it the forced vibration responses oscillate) and the horizontal dashed line is due to the differences of the vertical

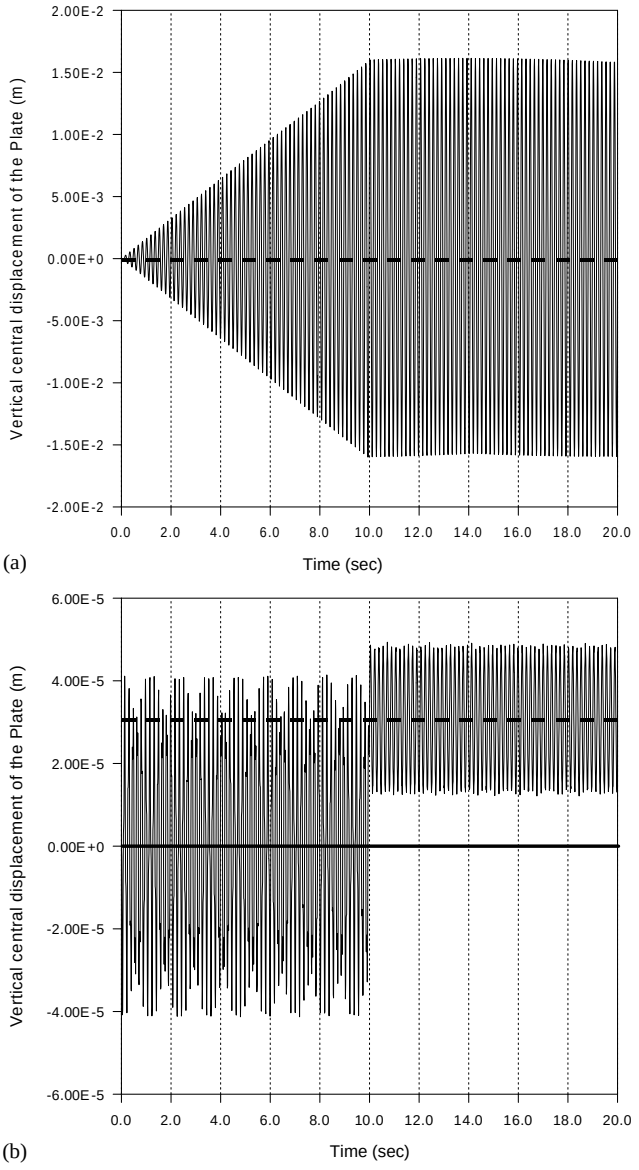

Fig. 6. Time histories for the vertical ($\bar{z}$) displacements of the centre G of H-plate subjected to a single concentrated sinusoidal force, $\bar{F}_{\bar{z},1}(t) = 10 \times \sin \Omega t$ N, moving along a circular path (of radius $r = 0.3$ m) with a constant rotating speed ω: (a) $\omega = \Omega = \omega_1 = 36.9741$ rad/s; (b) $\omega = \Omega = \omega_2 = 105.625$ rad/s.

($\bar{z}$) static deflections of centre G of the H-plate arising from different acting positions of the single moving load $\bar{F}_{\bar{z},1}(t)$. It is noted that the vertical ($\bar{z}$) central displacement corresponding to the horizontal dashed line represents the static equilibrium position of centre G of the H-plate due to applying on the plate the moving load $\bar{F}_{\bar{z},1}(t)$ located at the instantaneous position $[\bar{C}^{(s)}_{\bar{x},1}(10), \bar{C}^{(s)}_{\bar{y},1}(10)] = [1.234, 0.687] \neq [1.3, 0.5]$ given by Eq. (19) and with the instantaneous magnitude $\bar{F}_{\bar{z},1}(10) = 6.248$ N given by Eq. (20).

6.3. Influence of supporting conditions of the rectangular plate

All the conditions in this subsection are exactly the same as those in the last subsection except that the H-plate is replaced by the C-plate and both the rotating speed ω and the forcing frequency Ω relating to the moving force $\bar{F}_{\bar{z},1}(t)$ are equal to the first and second natural frequencies of the C-plate, ω_1 and ω_2.

Fig. 7(a) shows the time history for the vertical ($\bar{z}$) central displacement of the C-plate when $\omega = \Omega = \omega_1 = 13.6396\,\text{Hz} = 85.657\,\text{rad/s}$ and Fig. 7(b) shows that when $\omega = \Omega = \omega_2 = 21.9251\,\text{Hz} = 137.689\,\text{rad/s}$. Because the lowest two mode shapes of the C-plate are similar to the corresponding ones of the H-plate as one may see from Figs. 4 and 5, the time histories of the C-plate shown in Fig. 7 are also similar to the corresponding ones of the H-plate shown in Fig. 6.

From the numerical results of the last and the present subsections, one may conclude that the influence of the rotating speed (ω) and forcing frequency (Ω) of the moving force $F_{\bar{z},1}(t)$ on the dynamic responses of the rectangular plate is as significant as the supporting conditions of the plate. Hence, if a rotating mechanism like the one shown in Fig. 1 is designed, in addition to the supporting conditions of the plate, one must also pay attention to the rotating speed (ω) and the forcing frequency (Ω) of the moving force to avoid the occurrence of resonance.

6.4. Static deflections of the H-plate due to multiple moving loads

From the last subsections one sees that the magnitudes of the forced vibration responses of the rectangular plate due to the moving loads have a close relationship with the static equilibrium position of the plate induced by the loads statically stayed on the plate. Thus, the vertical ($\bar{z}$) static deflections for the centre G of the H-plate due to the moving loads with rotating speed $\omega = 0$ and various initial angles θ_0 (for $\bar{F}_{\bar{z},1}$) are studied in this subsection. If the number of moving loads is $k = 3$ and the magnitude of each load is equal to 4 N (i.e., $\bar{F}_{\bar{z},i} = F_g/3 = 4\,\text{N}$, $i = 1-3$), then the deflection curves for the three cases with radii of the circular paths $r = 0.2$, 0.3 and 0.4 m are, respectively, shown in Fig. 8. Where the ordinate denotes the vertical central static deflections of the H-plate and the abscissa the values of the initial angles θ_0 for the first moving load $\bar{F}_{\bar{z},1}$. It is noted that different value of θ_0 implies different relative position between the moving loads and the rectangular plate and will induce different static deflections of the centre G of the plate. From the figure one sees that the smaller the radius of the circular path,r, the larger the vertical ($\bar{z}$) static deflections of the centre G of the H-plate. It is evident that this result agrees with the actual situation. For convenience, the boundaries for the variations of each deflection curve are indicated by a dashed line (- - -) and a solid line (—) and assigned to D_i and S_i, respectively, and the domain between each pair of dashed line and solid line is called a *static deflection region*, where D_i denotes the dashed line and S_i the solid line, while $i = 1$ is for the radius of circular path $r = 0.2$ m, $i = 2$ is for $r = 0.3$ m and $i = 3$ is for $r = 0.4$ m.

6.5. Influence of the radius of the circular path

When the three forces mentioned in the last subsection move, with angular velocity $\omega = 12.56\,\text{rad/s}$, along the circular paths with radii $r = 0.2, 0.3$ and 0.4 m, respectively, the time histories for the vertical ($\bar{z}$) displacements of centre G of H-plate are shown in Fig. 9. Where the

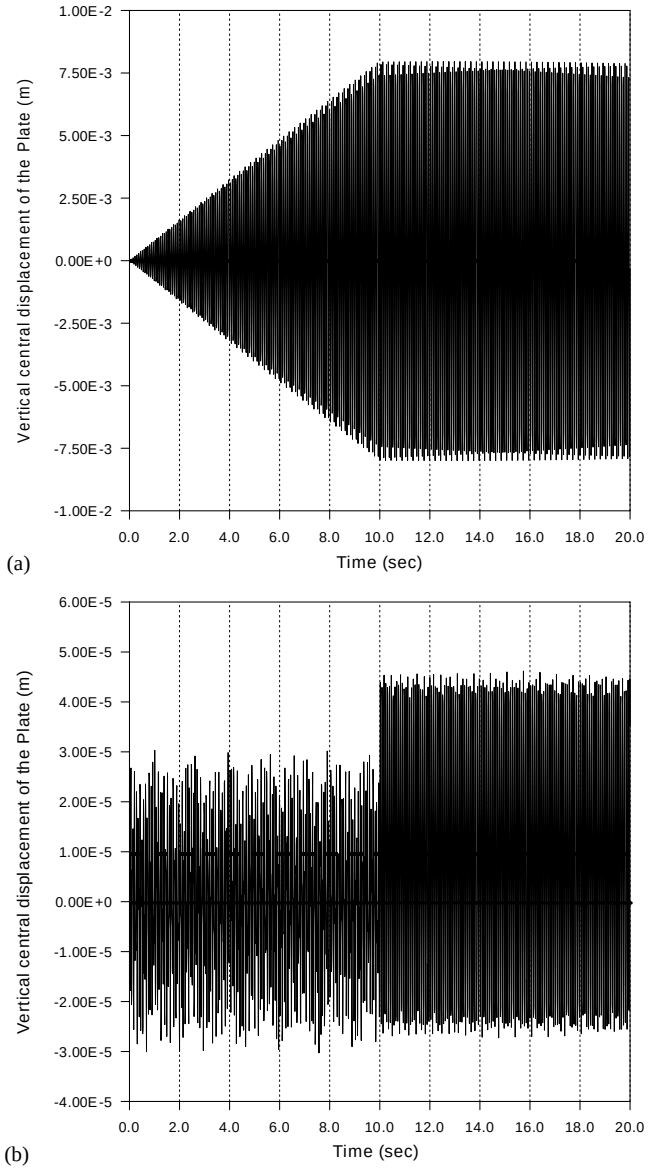

Fig. 7. Time histories for the vertical ($\bar{z}$) displacements of the centre G of C-plate subjected to a single concentrated sinusoidal force, $\bar{F}_{\bar{z},1}(t) = 10 \times \sin \Omega t$ N, moving along a circular path (of radius $r = 0.3$ m) with a constant rotating speed ω: (a) $\omega = \Omega = \omega_1 = 85.657$ rad/s; (b) $\omega = \Omega = \omega_2 = 137.689$ rad/s.

responses for the case of $r = 0.2$ m are represented by the thin solid curve (——), those for the case of $r = 0.3$ m by the thin solid curve with rectangles (—◇—), and those for the case of $r = 0.4$ m by the thin solid curve with stars (—☆—), besides, each pair of horizontal dashed line and solid line (D_i and S_i, $i = 1, 2, 3$) denotes the upper and lower boundary lines for each associated *static deflection region* shown in Fig. 8. From Fig. 9 one sees that the vertical ($\bar{z}$) central displacements of the plate due to forced vibrations (during $0 \leqslant t \leqslant 10$ s) induced by the multiple loads moving along

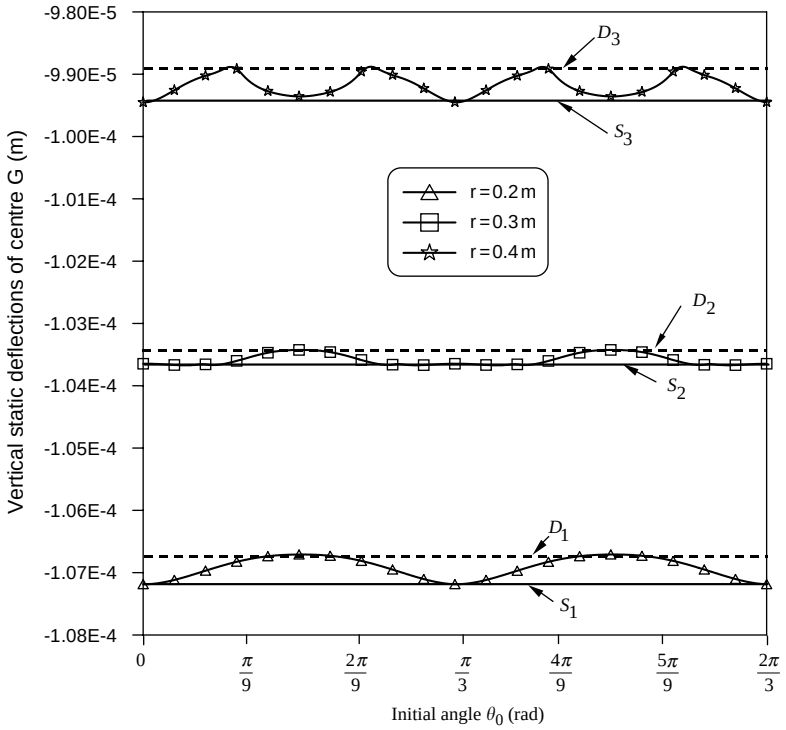

Fig. 8. Influence of initial angle θ_0 on the vertical static deflections of the centre G of the H-plate. D_1, S_1: upper and lower boundary lines for $r = 0.2$ m; D_2, S_2: upper and lower boundary lines for $r = 0.3$ m; D_3, S_3: upper and lower boundary lines for $r = 0.4$ m.

a specified circular path, with radius $r = 0.2$, 0.3 or 0.4 m, oscillate with respect to the static deflection region with a small downward shift, while those due to free vibrations induced by the three loads statically stayed on the plate (after $t \geqslant 10$ s) oscillate with respect to the associated horizontal solid line S_1, S_2 or S_3. Since the three identical moving loads, $\bar{F}_{\bar{z},i}$ $(i = 1, 2, 3)$, are equally spaced (with constant spacing angle $\alpha = 360^\circ/3 = 120^\circ$) and their rotating speed is $\omega = 12.56$ rad/s=2 Hz, the three loads return to their original positions at the instant of time $t = 10$ s. For this reason, the free vibration responses after 10 s (i.e., $t > 10$ s) oscillate with respect to the associated horizontal solid line (S_1, S_2 or S_3).

6.6. *Influence of number of moving forces*

For the H-plate subjected to multiple identical loads, $\bar{F}_{\bar{z},i} = F_g/k$ $(i = 1-k)$, moving along a circular path of radius $r = 0.3$ m, if both the summation of the magnitudes, F_g, and the rotating speed, ω, for all the moving loads are constant and respectively given by $F_g = \sum_{i=1}^{k} \bar{F}_{\bar{z},i} = 12$ N and $\omega = 12.56$ rad/s=2 Hz, then the influence of number of moving loads, k, on the vertical ($\bar{z}$) central displacements of the H-plate is shown in Fig. 10. Where the dashed line (- - -) and the solid line (—), respectively, represent the vertical ($\bar{z}$) central displacements of the H-plate due to six and seven moving forces, while the curve with circles (—●—) and the curve with triangles (—▲—),

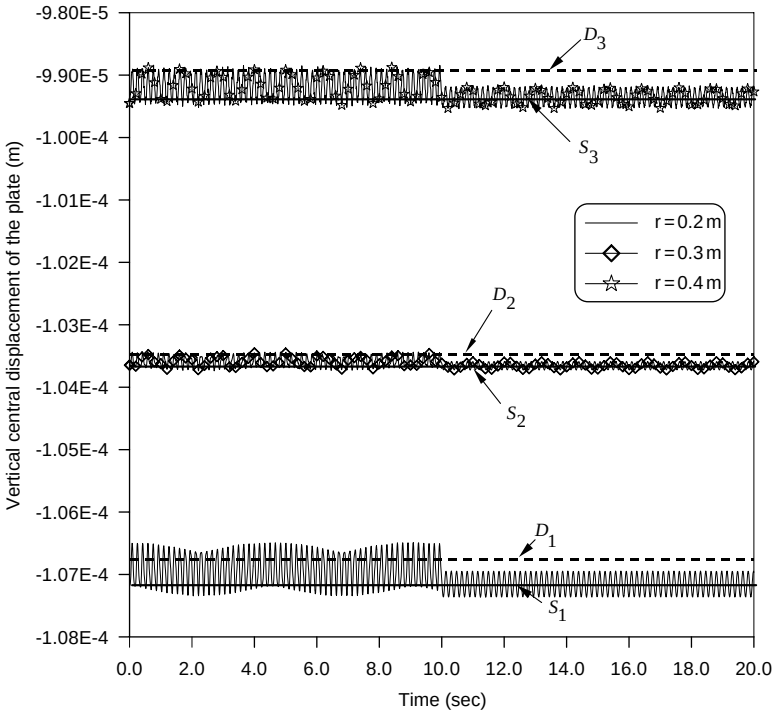

Fig. 9. Time histories for the vertical ($\bar{z}$) displacements of the centre G of H-plate subjected to three identical constant forces, $\bar{F}_{\bar{z},i} = F_g/k = 12/3 = 4\,\mathrm{N}$ ($i = 1-3$), moving along a circular path with different radii $r = 0.2$, 0.3 and 0.4 m. The rotating speed for the moving forces is $\omega = 12.56\,\mathrm{rad/s} = 2\,\mathrm{Hz}$.

respectively, represent those due to eight and nine moving forces. From the figure it is found that even if the summation for the magnitudes of all the moving loads is constant and the distribution for all the moving loads along the circular path is uniform, the vibration amplitudes of the centre G of H-plate vary with the total number k of the moving loads.

7. Conclusions

1. By means of the formulations for calculating the instantaneous overall nodal forces (and moments) of a rectangular plate subjected to multiple forces moving along a circular path, presented in this paper, one may solve the title problem with the finite element method. The presented formulations are also available for the case of a single moving force.
2. For a rectangular plate subjected to a single force moving along a circular path, the rotating speed and the forcing frequency are two key factors affecting the dynamic responses of the rectangular plate. Numerical example shows that the responses of the plate become predominant if both the rotating speed and the forcing frequency are very close to certain lowest natural frequencies of the rectangular plate, particularly to the fundamental one.
3. For a rectangular plate subjected to multiple loads moving along a circular path, there exist an upper limit and lower limit for the vertical ($\bar{z}$) central static deflections of the plate when the

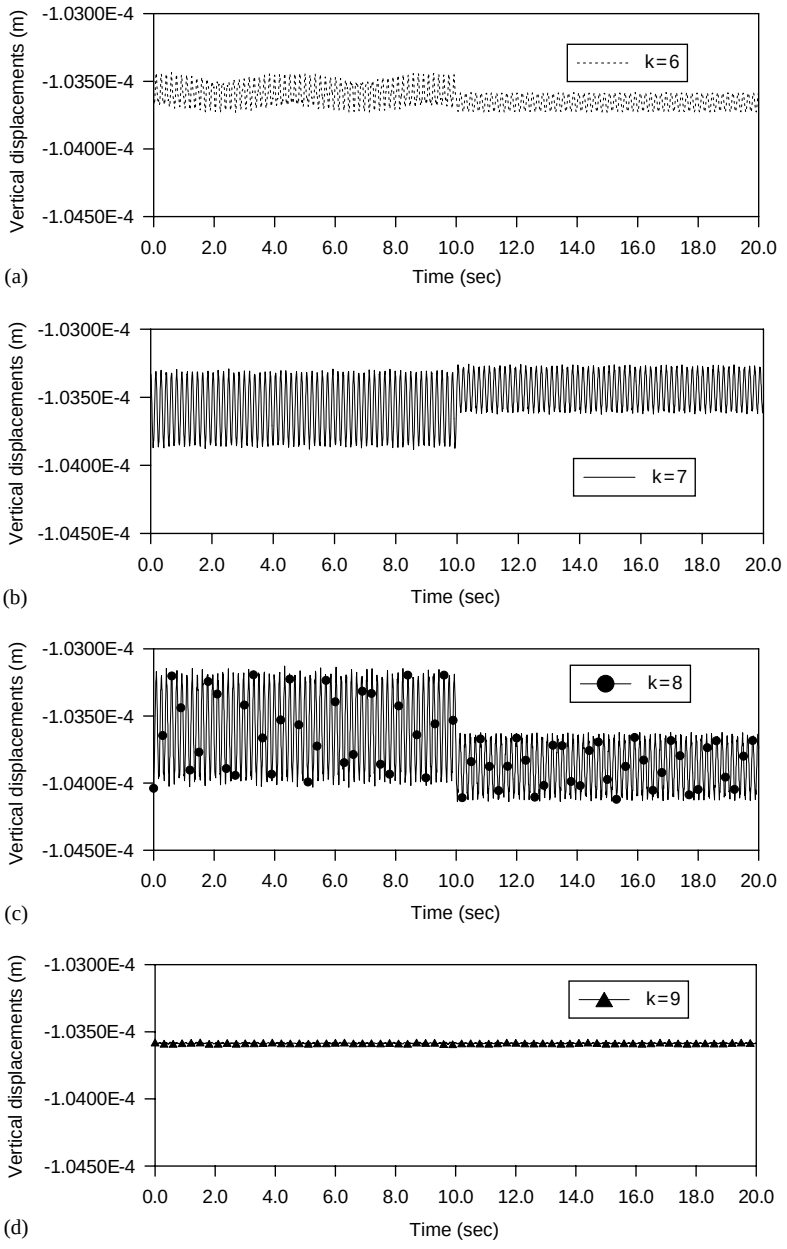

Fig. 10. Time histories for the vertical ($\bar{z}$) displacements of the centre G of H-plate subjected to (a) $k = 6$, (b) $k = 7$, (c) $k = 8$ and (d) $k = 9$ identical constant forces, $\bar{F}_{\bar{z},i} = F_g/k = 12/k$ N (i=1–k), moving along a circular path (of radius $r = 0.3$ m) with rotating speed $\omega = 12.56$ rad/s.

moving loads stay arbitrarily. If the domain between the upper and lower boundary lines is called the *static deflection region*, then the vertical ($\bar{z}$) central displacements of the plate due to forced vibrations induced by the multiple loads moving along a circular path will oscillate with

respect to the *static deflection region* with a small downward shift, while those induced by free vibrations of the loads stay arbitrarily will oscillate with respect to the vertical central static deflection due to the loads located at the positions where they stay and with the force magnitudes at that instant of time. This conclusion is also available for a single moving load.

4. For a rectangular plate undergoing multiple identical loads moving along a circular path with radius r, if both the summation of magnitudes, F_g, and the number of the moving loads, k, remain unchanged, then the vertical central static deflection of the plate decreases with the increase of radius of the circular path.
5. If a rectangular plate is subjected to the multiple identical loads moving along a circular path with radius r, the vertical ($\bar{z}$) central displacements of the plate vary with the number of moving loads even if the summation for the magnitude of all the moving loads (F_g) is constant and the distribution for all the moving loads along the circular path is uniform.

References

[1] Y.H. Lin, M.W. Trethewey, Finite element analysis of elastic beams subjected to moving dynamic loads, Journal of Sound and Vibration 136 (1990) 323–342.
[2] Y.H. Lin, M.W. Trethewey, H.M. Reed, J.D. Shawley, S.J. Sager, Dynamic modelling and analysis of a high-speed precision drilling machine, Journal of Vibration and Acoustics 112 (1990) 355–365.
[3] J. Hino, T. Yoshimura, N. Ananthanarayana, Vibration analysis of non-linear beams subjected to a moving load using the finite element method, Journal of Sound and Vibration 100 (1985) 477–491.
[4] T. Yoshimura, J. Hino, N. Ananthanarayana, Vibration analysis of a non-linear beam subjected to moving loads by using the Galerkin method, Journal of Sound and Vibration 104 (1986) 179–186.
[5] J. Hino, T. Yoshimura, K. Konishi, N. Ananthanarayana, A finite element method prediction of the vibration of a bridge subjected to a moving vehicle load, Journal of Sound and Vibration 96 (1984) 45–53.
[6] T.P. Chang, Y.N. Liu, Dynamic finite element analysis of a non-linear beam subjected to a moving load, Journal of Solids and Structures 33 (1996) 1673–1688.
[7] J.S. Wu, C.W. Dai, Dynamic responses of multi-span non-uniform beam due to moving loads, Journal of Structural Engineering 113 (1987) 458–474.
[8] H.P. Lee, Dynamic response of a multi-span beam on one-side point constraints subject to a moving load, Computers & Structures 55 (1995) 615–623.
[9] D. Thambiratnam, Y. Zhuge, Dynamic analysis of beams on an elastic foundation subjected to moving loads, Journal of Sound and Vibration 198 (1996) 149–169.
[10] J.J. Wu, A.R. Whittaker, M.P. Cartmell, The use of finite element techniques for calculating the dynamic response of structures to moving load, Computers & Structures 78 (2000) 789–799.
[11] J.S. Wu, M.L. Lee, T.S. Lai, The dynamic analysis of a flat plate under a moving load by the finite element method, Journal for Numerical Methods in Engineering 24 (1987) 743–762.
[12] E. Manoach, Dynamic response of elastoplastic mindlin plate by mode superposition method, Journal of Sound and Vibration 162 (1993) 165–175.
[13] L. Frýba, Vibration of Solids and Structures under Moving Loads, Noordhoff International Publishing, The Netherlands, 1971.
[14] J.A. Gbadeyan, S.T. Oni, Dynamic behaviour of beams and rectangular plates under moving loads, Journal of Sound and Vibration 182 (1995) 677–695.
[15] Y.H. Lin, Comments on "Dynamic behaviour of beams and rectangular plates under moving loads", Journal of Sound and Vibration 200 (1997) 721–728.
[16] H. Takabatake, Dynamic analysis of rectangular plates with stepped thickness subjected to moving loads including additional mass, Journal of Sound and Vibration 213 (1998) 829–842.

[17] S. Marchesiello, A. Fasana, L. Garibaldi, B.A.D. Piombo, Dynamics of multi-span continuous straight bridges subjected to multi-degrees of freedom moving vehicle excitation, Journal of Sound and Vibration 224 (1999) 541–561.
[18] X.Q. Zhu, S.S. Law, Identification of vehicle axle loads from bridge dynamic responses, Journal of Sound and Vibration 236 (2000) 705–724.
[19] R.E. Rossi, R.H. Gutierrez, P.A.A. Laura, Forced vibrations of rectangular plates subjected to harmonic loading distributed over a rectangular subdomain, Ocean Engineering 28 (2001) 1575–1584.
[20] M.R. Shadnam, M. Mofid, J.E. Akin, On the dynamic response of rectangular plate, with moving mass, Thin-Walled Structures 39 (2001) 797–806.
[21] J.J. Wu, Use of beamplate model for the dynamic analysis of rectangular plates under moving forces, Technique report, Department of Marine Engineering, National Kaohsiung Institute of Marine Technology, Kaohsiung, Taiwan, 2001.
[22] R.W. Clough, J. Penzien, Dynamics of Structures, McGraw-Hill, New York, 1993.
[23] G.H. Golub, R. Underwood, J. H. Wilkinson The Lanczos algorithm for the symmetric Ax = Lambda * Bx problem, Computer Science Department, Stanford University, 1972.
[24] K.J. Bathe, Finite Element Procedure in Engineering Analysis, Prentice-Hall, Englewood Cliffs, NJ, 1982.